Therapeutic Potential of Nrf2 Activators in Streptozotocin-Induced Diabetic Nephropathy

Hongting Zheng,[1,2] Samantha A. Whitman,[1] Wei Wu,[1,2] Georg T. Wondrak,[1] Pak K. Wong,[3] Deyu Fang,[4] and Donna D. Zhang[1]

OBJECTIVE—To determine whether dietary compounds targeting NFE2-related factor 2 (Nrf2) activation can be used to attenuate renal damage and preserve renal function during the course of streptozotocin (STZ)-induced diabetic nephropathy.

RESEARCH DESIGN AND METHODS—Diabetes was induced in $Nrf2^{+/+}$ and $Nrf2^{-/-}$ mice by STZ injection. Sulforaphane (SF) or cinnamic aldehyde (CA) was administered 2 weeks after STZ injection and metabolic indices and renal structure and function were assessed (18 weeks). Markers of diabetes including blood glucose, insulin, polydipsia, polyuria, and weight loss were measured. Pathological alterations and oxidative damage in glomeruli were also determined. Changes in protein expression of the Nrf2 pathway, as well as transforming growth factor-β1 (TGF-β1), fibronectin (FN), collagen IV, and p21/WAF1Cip1 (p21) were analyzed. The molecular mechanisms of Nrf2-mediated protection were investigated in an in vitro model using human renal mesangial cells (HRMCs).

RESULTS—SF or CA significantly attenuated common metabolic disorder symptoms associated with diabetes in $Nrf2^{+/+}$ but not in $Nrf2^{-/-}$ mice, indicating SF and CA function through specific activation of the Nrf2 pathway. Furthermore, SF or CA improved renal performance and minimized pathological alterations in the glomerulus of STZ-$Nrf2^{+/+}$ mice. Nrf2 activation reduced oxidative damage and suppressed the expression of TGF-β1, extracellular matrix proteins and p21 both in vivo and in HRMCs. In addition, Nrf2 activation reverted p21-mediated growth inhibition and hypertrophy of HRMCs under hyperglycemic conditions.

CONCLUSIONS—We provide experimental evidence indicating that dietary compounds targeting Nrf2 activation can be used therapeutically to improve metabolic disorder and relieve renal damage induced by diabetes. ***Diabetes*** **60:3055–3066, 2011**

Diabetic nephropathy is the leading cause of chronic kidney disease accounting for nearly 50% of all end-stage renal disease worldwide (1,2). Current therapies that aim to lower blood glucose are not effective in blocking renal damage, and cotreatment with renoprotective drugs often results in toxicity, limiting efficacy. Hence, there remains an urgent need to develop effective medicines to preserve normal renal function and to prevent or slow the progression of diabetic nephropathy.

Several mechanisms contribute to the onset and pathogenesis of diabetic nephropathy, including genetic and hemodynamic factors, oxidative stress, and cytokine signaling (rev. in 1). Although diabetic nephropathy involves many renal cell types, mesangial activation by cytokines under hyperglycemic conditions plays an important role in the progression of diabetic nephropathy (2,3). The cytokine transforming growth factor-β1 (TGF-β1) is central to the profibrotic switch and activation of mesangial cell hypertrophy and matrix production and is upregulated in diabetic nephropathy (4,5). Previous interventions at the level of TGF-β1 ameliorated several pathological symptoms of diabetic nephropathy (6,7), indicating reduction of hypertrophy and extracellular matrix (ECM) accumulation in the kidney may be a viable therapeutic avenue.

The transcription factor NFE2-related factor 2 (Nrf2) is an emerging therapeutic target for several diseases including cancer (8), neurodegenerative diseases (9), pulmonary fibrosis (10), and diabetes (11). Nrf2 regulates expression of numerous genes through antioxidant response elements in their promoters to neutralize free radicals and accelerate removal of environmental toxins (rev. in 12). Prior to cell stress (where basal levels of Nrf2 are low), activation of Nrf2 with low toxicity (dietary) compounds like sulforaphane (SF) from cruciferous vegetables and cinnamic aldehyde (CA), the key flavor compound in cinnamon essential oil extracted from Cinnamomum zeylanicum and Cinnamomum cassia bark (U.S. Food and Drug Administration approved for use in food), can reduce disease onset or improve prognosis (13–18).

Using streptozotocin (STZ)-induced diabetic models, a protective role of Nrf2 against renal damage through mediation of free radicals was demonstrated (11,19). Recently, evidence was introduced supporting the therapeutic potential of Nrf2 activation in diabetes (20–24), implicating control of oxidative stress in addition to regulation of inflammatory cytokines as methods of Nrf2 protection.

The current study aimed to explore the therapeutic potential of known dietary Nrf2 activators to slow the progression of diabetic nephropathy using an STZ-induced diabetic model. Our results demonstrate that SF or CA were able to ameliorate albuminuria and minimize renal damage induced by diabetes in an Nrf2-dependent fashion. Furthermore, our results describe an additional mechanism for Nrf2-mediated protection through the negative regulation of TGF-β1 and p21/WAF1Cip1 (p21). This study provides convincing experimental evidence that dietary compounds SF or CA may be used therapeutically to improve metabolic disorder and relieve renal damage induced by diabetes.

From the [1]Department of Pharmacology and Toxicology, University of Arizona, Tucson, Arizona; the [2]Department of Endocrinology, Xinqiao Hospital, Third Military Medical University, Chongqing, China; the [3]Department of Aerospace and Mechanical Engineering, University of Arizona, Tucson, Arizona; and the [4]Department of Pathology, School of Medicine, Northwestern University, Chicago, Illinois.

Corresponding author: Donna Zhang, dzhang@pharmacy.arizona.edu.

Received 13 June 2011 and accepted 31 July 2011.

DOI: 10.2337/db11-0807

See accompanying commentary, p. 2683.

RESEARCH DESIGN AND METHODS

Chemicals, reagents, kits, and antibodies. CA, STZ, and *tert*-butylhydroquinone (tBHQ), Periodic Acid-Schiff (PAS) kit, and Trichrome stain (Masson) kit were purchased from Sigma (St. Louis, MO). Sulforaphane (SF, L-isomer) was obtained from LKT laboratories (St. Paul, MN). Blood glucose levels were measured using AlphaTRAK system (Abbott Laboratory, North Chicago, IL). Insulin was detected using mouse insulin ELISA kit (Millipore, St. Charles, MO). Urine was collected for analysis in metabolic cages (Hazleton Systems Inc., Aberdeen, MD). Urinary albumin or urinary creatinine was measured by ELISA (Bethyl Laboratories, Houston, TX; Exocell, Philadelphia, PA). Antibodies for immunoblot and immunohistochemical (IHC) analysis included anti-7,8-dihydro-8-oxo-2′-deoxyguanosine (8-oxo-dG) (Trevigen, Gaithersburg, MD); anti-fibronectin (FN) (Calbiochem, San Diego, CA); anti-collagen IV (Abcam, San Francisco, CA); anti-Ki67 (Vector Laboratories, Burlingame, CA); and anti-Nrf2, NAD(P)H dehydrogenase, quinone 1 (NQO1), γ-glutamylcysteine synthetase (γ-GCS), p21, TGF-β1, and β-actin (Santa Cruz Biotechnology, Santa Cruz, CA).

Animal treatment. $Nrf2^{+/+}$ and $Nrf2^{-/-}$ C57BL/6 mice (described previously in 25) were obtained through breeding of $Nrf2^{+/-}$. All animals received water and food ad libitum. Eight-week-old mice received either sodium citrate (control) or STZ (50 mg/kg, pH 4.5, dissolved in sodium citrate) through intraperitoneal (i.p.) injection for 5 consecutive days. Two weeks following STZ injection, fasting glucose levels (4-h fast) were measured, and mice with a fasting glucose level above 250 mg/dL were considered diabetic and used for this study. Mice were randomly allocated into four groups ($n = 8$ per group) to receive treatment: *1*) control = corn oil, *2*) CA1 = 25 mg/kg CA, *3*) CA2 = 50 mg/kg CA, *4*) SF = 12.5 mg/kg SF. Each of the compounds was administered (i.p., diluted in corn oil) three times per week for 16 weeks. Doses of SF and CA were guided by published literature (14–16) and tested in pilot studies to ensure Nrf2 activation within 48 h after i.p. injection. At 18 weeks, mice were killed and the kidney, blood, and urine were isolated for analysis.

Renal morphology assessment. Tissue sections from paraffin-embedded kidney were stained with hematoxylin-eosin (HE), periodic acid Schiff (PAS), and Masson's trichrome. Glomerulosclerotic index was assessed on PAS-stained tissue sections using a five-grade method described previously (11). The thickness of the glomerular basement membrane (GBM) was measured by electron microscopy (Arizona Health Sciences Center, Imaging Core, University of Arizona, Tucson, AZ). Images were captured by CCD camera system (Advanced Microscopy Techniques, Woburn, MA), and thickness was measured using the ruler function of the software. Average thickness for each mouse was calculated from 50 measurements obtained from different sites of GBM.

IHC analysis and tissue oxidative DNA damage. IHC analysis was performed as described previously (26). Oxidative DNA damage was measured by the amount of 8-oxo-dG, using two methods: *1*) deparaffinized kidney sections were treated with proteinase K (10 μg/mL), RNase A (100 μg/mL), and 2N HCl then stained by IHC with an anti-8-oxo-dG antibody and *2*) urinary 8-oxo-dG was measured by sampling 50 μl urine against standards generated from 0.7067 mmol/L stock using liquid chromatography-mass spectometry/mass spectormetry (Arizona Cancer Center Proteomics Core) according to published protocols (27,28).

Cell culture, reactive oxygen species detection, and small interfering RNA transfection. HRMCs were purchased and maintained according to distributor guidelines from ScienCell Research Laboratories (Carlsbad, CA). For experiments, HRMCs were starved in serum- and supplement-free Dulbecco's modified Eagle's medium (DMEM) containing normal glucose (NG, 5.5 mmol/L) for 24 h. Cells were then either maintained in serum-free NG DMEM (plus 19.5 mmol/L mannitol to control for osmolality) or switched to serum-free high glucose (HG, 25 mmol/L) DMEM supplied with supplement, along with treatment (SF [1.25 μmol/L, empirically determined]), or CA (5 μmol/L [29]), or tBHQ (6.25 μmol/L, empirically determined). Cells were cultured in HG with or without treatments for 48 or 96 h. Reactive oxygen species (ROS) in cultured HRMCs were detected using dichlorodihydrofluorescein diacetate (Invitrogen, Carlsbad, CA), and the fluorescence intensity was measured by flow cytometry. Small interfering RNAs (siRNAs) specific for Nrf2, Keap1, or p21, as well as HiPerfect transfection reagent were purchased from Qiagen (Valencia, CA), and transfection of siRNAs was performed according to manufacturer's instructions.

Immunoblot analysis, cell proliferation and death, hypertrophy, and cell imaging. Tissue lysates were prepared as previously described (11). Protein concentration was determined using Quant-IT Protein Assay (Invitrogen). Cultured cells were lysed in sample buffer (50 mmol/L Tris–HCl [pH 6.8], 2% SDS, 10% glycerol, 100 mmol/L dithiothreitol, 0.1% bromophenol blue). Total lysates were loaded and electrophoresed through SDS–polyacrylamide gels and subjected to immunoblot analysis. The rate of cell proliferation was measured two ways: *1*) 8,000 HRMCs per well were seeded in NG or HG media with or without Nrf2 activator and cell growth was monitored for 96 h using the xCELLigence system (Roche) (30) and *2*) detection of Ki67 using indirect immunofluorescence as described previously (31). The *In Situ* Cell Death Detection Kit (Roche) was used according to manufacturer's instructions to detect apoptosis. Cell size was measured by forward light scatter using flow cytometry and the average area per cell in green fluorescent protein (GFP)-transfected living cells as described below. Cells were transfected with GFP and maintained in NG or HG media with or without an Nrf2 activator. Fluorescent images were taken using a Zeiss Observer.Z1 microscope. Cell size was calculated using the Slidebook 4.2.0.11 software (Intelligent Imaging Innovations, Inc., Denver, CO).

Statistical analysis. Results are expressed as mean ± SD. Statistical tests were performed using SPSS 10.0. Unpaired Student t tests were used to compare the means of two groups. One-way ANOVA was applied to compare the means of three or more groups. $P < 0.05$ was considered to be significant.

RESULTS

Activation of Nrf2 by SF or CA improves metabolic disorder in an STZ-induced diabetic model. The effectiveness of dietary Nrf2 activators in alleviating metabolic disorder was assessed in the STZ-induced diabetic model in both $Nrf2^{+/+}$ and $Nrf2^{-/-}$ mice, and common metabolic disorder indices associated with diabetes were measured. In response to STZ, mice showed significantly increased blood glucose levels (Fig. 1*A*), reduced weight gain (Fig. 1*B*), increased urine production (Fig. 1*C*), and increased water uptake (Fig. 1*D*). Importantly, treatment of diabetic animals with SF or CA significantly alleviated all indices of metabolic dysfunction in $Nrf2^{+/+}$ animals only, demonstrating the Nrf2-dependent response to SF and CA. In addition, STZ injection decreased insulin levels significantly, which was unaltered by treatment with SF or CA regardless of genotype (Fig. 1*E*), indicating that the protective effects of SF and CA were not insulin dependent. Since treatment with Nrf2 activators began 2-weeks post-STZ injection, after the pancreatic β-cells had been destroyed and diabetes was established, we did not expect SF or CA treatments to influence circulating insulin levels in this study. Taken together, these results indicate that SF or CA treatment significantly attenuated metabolic disorder induced by STZ, and that this protective effect was independent of circulating insulin levels.

SF or CA alleviates renal damage induced in the STZ diabetic model. To investigate the therapeutic effects of Nrf2 activation on improvement of kidney performance in the STZ diabetic model, functional and pathological changes of the kidney were measured. The ratio of kidney weight-to-body weight was higher in all STZ-injected groups compared with untreated, which was significantly attenuated by treatment with SF or CA in $Nrf2^{+/+}$ mice (Fig. 2*A*). Next, as indices of albuminuria, both urinary albumin excretion (UAE) and the urine albumin-to-creatinine ratio (UACR) were determined at 0, 10, and 18 weeks. Injection with STZ increased UAE and UACR in all treated groups; however, this increase was blunted by SF or CA treatment in $Nrf2^{+/+}$ mice but not $Nrf2^{-/-}$ mice (Fig. 2*B* and *C*). These results demonstrate that SF or CA is able to improve albuminuria in $Nrf2^{+/+}$ diabetic mice.

In agreement with the urinalysis, SF or CA treatment alleviated the pathological alterations of the glomerulus as revealed by histological examination. Glomerular lesions, including K-W (Kimmelstiel Wilson) nodules, were observed in HE-stained tissue sections from STZ-injected mice (Fig. 2*D*, HE panel, *arrows*). Treatment with SF or CA2 effectively restored the normal morphology of glomeruli in $Nrf2^{+/+}$ but not $Nrf2^{-/-}$ mice (Fig. 2*D*, HE panel). Glycogen deposition in the glomeruli was measured by PAS staining and scored to indicate the severity of glomerulosclerosis. PAS staining

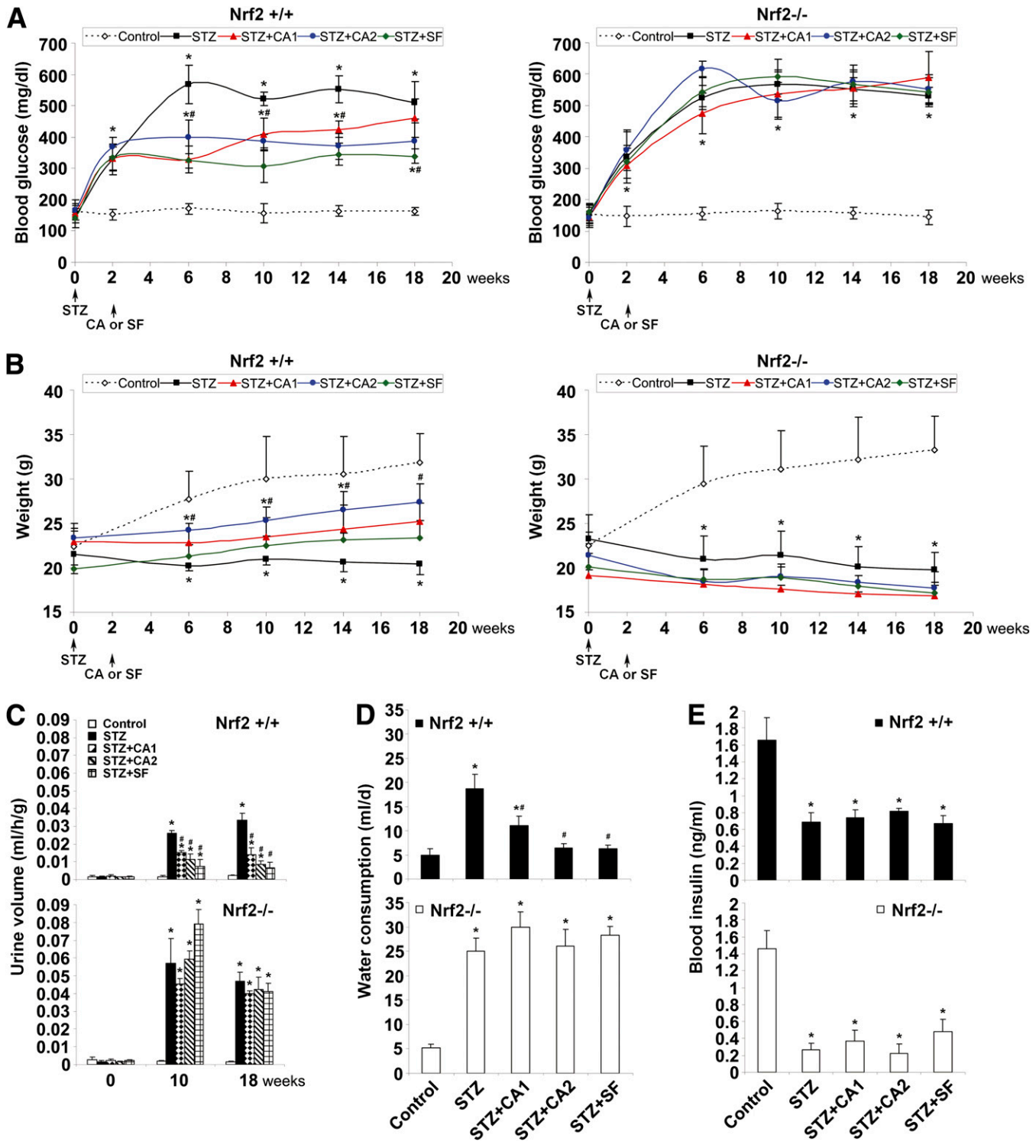

FIG. 1. Activation of Nrf2 by SF or CA improves metabolic disorder in an STZ-induced diabetic model. *A*: The average level of blood glucose in each animal group is plotted. STZ animals (■) showed significant increase in blood glucose levels in both Nrf2$^{+/+}$ (*left panel*) and Nrf2$^{-/-}$ animals (*right panel*). SF (◆) and CA (●,▲) treatment significantly reduced blood glucose in Nrf2$^{+/+}$ only. *B*: Body weights of Nrf2$^{+/+}$ (*left panel*) and Nrf2$^{-/-}$ (*right panel*) animals are displayed. STZ injection (■) caused significant decrease in weight in all animals that was recovered by SF (◆) and CA (●,▲) treatment in Nrf2$^{+/+}$ only. *C*: Urine output from Nrf2$^{+/+}$ (*top panel*) and Nrf2$^{-/-}$ (*bottom panel*) animals is shown. STZ injection increased urine output in Nrf2$^{+/+}$ animals (*top panel*) with a more significant increase in Nrf2$^{-/-}$ animals (*bottom panel*). SF and CA treatment significantly reduced urine output at 10 and 18 weeks in Nrf2$^{+/+}$ only. *D*: Water consumption in the last 24 h before these mice were killed is reported. STZ injection increased water intake in both Nrf2$^{+/+}$ (*top panel*) and Nrf2$^{-/-}$ (*bottom panel*) animals. SF and CA treatment significantly reduced consumption in Nrf2$^{+/+}$ only. *E*: Blood insulin is displayed. STZ injection decreased blood insulin levels in both Nrf2$^{+/+}$ (*top panel*) and Nrf2$^{-/-}$ (*bottom panel*) animals. SF and CA did not affect insulin levels in any animals. Data in *A–E* are expressed as mean ± SD (n = 8). *P < 0.05 compared with control. #P < 0.05 dietary treatment compared with STZ alone. (A high-quality color representation of this figure is available in the online issue.)

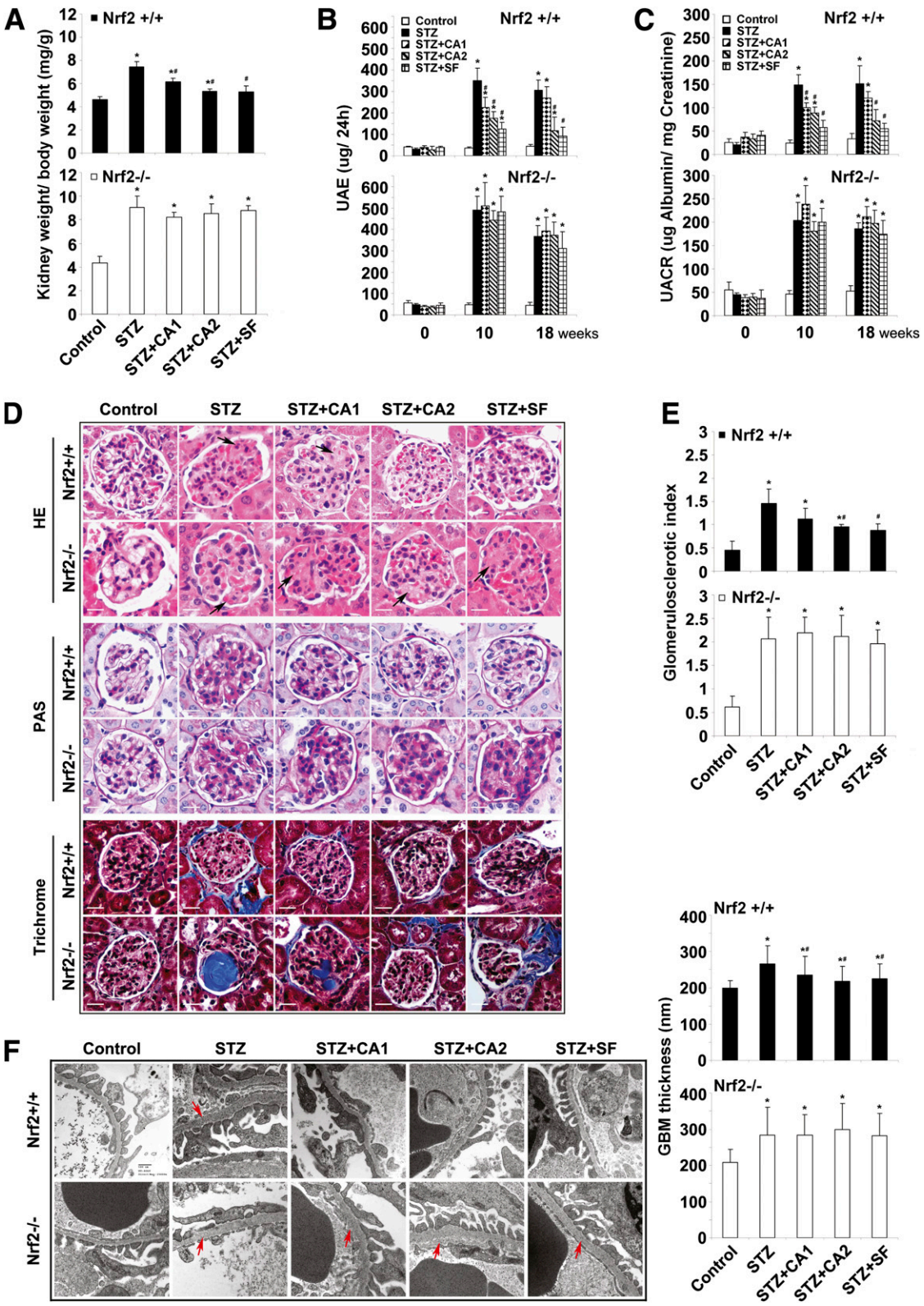

FIG. 2. SF or CA alleviates renal damage induced in the STZ-diabetic model. *A*: Kidney-to-body weight ratios are provided. STZ injection increased weight ratios in both Nrf2$^{+/+}$ (*top panel*) and Nrf2$^{-/-}$ (*bottom panel*) animals, which could be significantly reduced by SF and CA treatment in Nrf2$^{+/+}$ only. *B* and *C*: Albuminuria is reported as measures of UAE (*B*) and UACR (*C*). STZ injection increased UAE and UACR in both Nrf2$^{+/+}$ (*top panels*) and Nrf2$^{-/-}$ (*bottom panels*) animals, which were significantly reduced by SF and CA treatment in Nrf2$^{+/+}$ only. Kidney tissue sections from each mouse were subjected to HE, PAS, and trichrome staining. *D*: A representative image from one mouse per group is shown. *E*: PAS-stained tissues were used for semiquantitative scoring to get glomerulosclerotic index. A total of 30 glomeruli were scored for each mouse, and average scores with SD were shown (n = 3 per group). *F*: Electron microscopy of the GBM is displayed. GBM thickness was measured at 50 different sites (per animal) of the GBM in Nrf2$^{+/+}$ (*top panel*) and Nrf2$^{-/-}$ (*bottom panel*) animals and expressed as mean ± SD (n = 3 per group). Data in *A–C* are expressed as mean ± SD (n = 8). *P < 0.05 compared with control. #P < 0.05 dietary treatment compared with STZ alone. (A high-quality color representation of this figure is available in the online issue.)

showed STZ-induced glomerulosclerosis, which was significantly improved in SF- or CA2-treated $Nrf2^{+/+}$ but not $Nrf2^{-/-}$ mice (Fig. 2*D*, PAS panel, and Fig. 2*E*). Since ECM deposition is another hallmark of glomerulosclerosis, collagen was visualized using Masson's trichrome staining. STZ treatment resulted in collagen accumulation inside glomeruli or in the periglomerular area, which was reduced in SF- or CA-treated $Nrf2^{+/+}$ but not $Nrf2^{-/-}$ groups (Fig. 2*D*, trichrome panel). As an independent criterion for glomerulosclerosis, thickening of the GBM was measured by electron microscopy (Fig. 2*F*). STZ injection increased thickness of the GBM, which was reverted to control by SF or CA treatment only in $Nrf2^{+/+}$ mice (Fig. 2*F*). These results clearly demonstrate the ability of SF and CA treatment to attenuate STZ-induced pathological alterations both in renal function and structure during the progression of diabetic nephropathy.

SF- or CA-induced activation of the Nrf2 pathway confers protection against renal oxidative damage. Next, activation of Nrf2, its downstream targets, and oxidative damage in the kidney were assessed to demonstrate that the beneficial effect of SF or CA against renal damage is attributed to activation of the Nrf2 pathway and thus reduction of oxidative damage. Expression of Nrf2 and Nrf2 downstream targets NQO1 and γ-GCS was slightly increased after STZ injection, indicating induction of the Nrf2 pathway by renal oxidative stress. As expected, treatment with SF and CA markedly increased the protein levels of Nrf2, NQO1, and γ-GCS (Fig. 3*A* and *B*). Importantly, SF or CA treatment significantly reduced oxidative damage in the $Nrf2^{+/+}$ kidney, as measured by the formation of 8-oxo-dG either locally in glomerular tissues or systemically from the urine (Fig. 3*C* and *D*). Treatment with SF or CA did not increase NQO1 or γ-GCS or reduce oxidative damage in $Nrf2^{-/-}$ mice. Collectively, these results indicate that the kidney of STZ-induced diabetic mice is under oxidative stress, and that the renal protection mediated by SF or CA in the diabetic model is, at least in part, derived from specific activation of the Nrf2-mediated antioxidant response and reduction of oxidative damage.

Activation of Nrf2 reduces TGF-β1, ECM deposition, and p21 expression. Given that treatment with SF or CA diminished renal disorders resulting from STZ-induced diabetes, the molecular mechanisms underlying Nrf2-dependent protection of the kidney by SF or CA were explored. Previously, our laboratory reported a negative association between Nrf2 and TGF-β1. In accordance with that report, the basal expression of TGF-β1 was higher in $Nrf2^{-/-}$ mice compared with $Nrf2^{+/+}$ mice (Fig. 4*A* and *B*). Diabetes induced by STZ significantly upregulated protein levels of TGF-β1 and its downstream effectors, FN, collagen IV, and p21, which were significantly abrogated by treatment with SF or CA in the $Nrf2^{+/+}$ animals only (Fig. 4*A* and *B*). Treatment with SF and CA in the $Nrf2^{-/-}$ mice did not alter TGF-β1, ECM, or p21, indicating that the negative regulation of TGF-β1 and subsequent downstream effectors (ECM and p21) observed with SF and CA treatment is Nrf2 dependent.

Activation of Nrf2 diminishes mesangial ROS generation under hyperglycemic conditions. Mesangial cells play a crucial role in dictating the function of glomeruli. To understand the molecular mechanism(s) by which activation of Nrf2 is able to preserve renal function during the progression of diabetic nephropathy, cultured primary HRMCs were used. HRMCs growing in NG (5.5 mmol/L) media were shifted to either NG (plus 19.5 mmol/L mannitol) or HG (25 mmol/L) media to mimic hyperglycemic conditions in the presence or absence of an Nrf2 activator. Similar to the results reported above in the animal model of STZ-induced diabetes, culturing HRMCs under hyperglycemic conditions also activated the Nrf2 pathway (Fig. 5*A* and *B*), presumably through oxidative stress.

To support the in vivo findings reported above, HRMCs grown in HG media were treated with SF, CA, and tBHQ, a well-characterized Nrf2 activator. As expected, higher Nrf2 expression and predominate nuclear localization of Nrf2 were observed in response to tBHQ, SF, or CA treatment, indicating activation of the Nrf2 pathway (Fig. 5*A*). Consistently, protein levels of Nrf2 were enhanced after 48-h incubation in HG media and further induced by tBHQ, SF, or CA treatment (Fig. 5*B*). Similarly, protein levels of Nrf2 downstream targets including NQO1, GCS, or Mrp2, were increased in response to HG and further enhanced by treatment with an Nrf2 activator (Fig. 5*B*). To test if HRMCs growing in HG media were under oxidative stress, the level of ROS was measured. Indeed, HRMCs growing in HG media had ROS levels approximately 3.5-fold higher compared with HRMCs growing in NG media (Fig. 5*C*). As predicted, activation of Nrf2 by tBHQ, SF, or CA reduced ROS levels significantly (Fig. 5*C*). These results demonstrate ROS generation as a likely source of mesangial cell damage in diabetes and further demonstrate the beneficial effects of Nrf2 pathway activation in combating oxidative stress.

High glucose–mediated mesangial cell growth inhibition and hypertrophy can be reversed by activation of Nrf2. As a chronic disease, diabetic nephropathy is characterized by sequential pathological changes including cell growth inhibition and glomerular hypertrophy. First, we measured cell growth rate of HRMCs in differential glucose media using the xCELLigence system. As expected, the growth curve for HRMCs growing in HG media fell below those either growing in NG or in HG and supplemented with an Nrf2 activator (Fig. 6*A*). No cell death was observed under any condition and staining with Ki67 showed that hyperglycemia inhibited cell proliferation, which was counteracted by activation of Nrf2 (Fig. 6*B*). Next, the size of HRMCs under NG and HG conditions were measured by two independent methods. First, forward light scattering analysis by flow cytometry revealed a dramatic shift in size distribution (Fig. 6*C*), indicating an increase in the size of HRMCs growing in HG compared with NG media. Conversely, the light scattering curves for HRMCs growing in HG media in the presence of an Nrf2 activator were completely shifted back to the left where they overlapped with the curve of NG cells (Fig. 6*C*). Second, HRMCs were transfected with GFP to mark the entire area of cells. Incubation of HRMCs in HG media resulted in an increase in cell size as measured by the average area per GFP^+ cell. The hypertrophy observed in HG media was suppressed by treatment with tBHQ, SF, or CA (Fig. 6*D*). Collectively, these results demonstrate that hyperglycemia induced cell growth inhibition, and hypertrophy can be attenuated by activation of the Nrf2 pathway.

Blockage of TGF-β1 by Nrf2 activation alleviates ECM production and p21-mediated mesangial cell growth inhibition and hypertrophy. To gain molecular understanding of how Nrf2 activation relieves HRMC hypertrophy and growth inhibition under hyperglycemic conditions, the expression of TGF-β1 and its downstream effectors

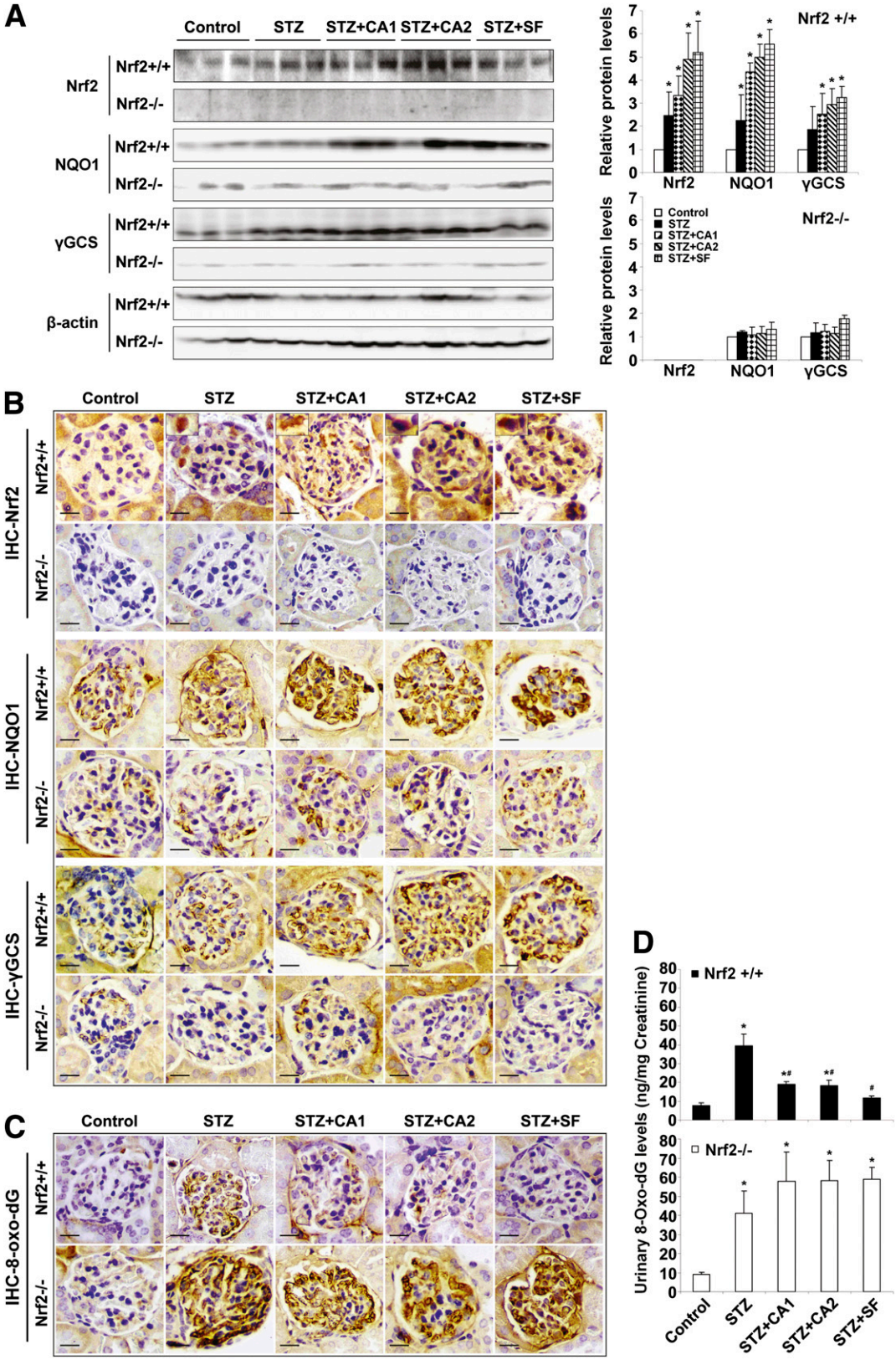

FIG. 3. SF- or CA-induced activation of the Nrf2 pathway confers protection against renal oxidative damage. *A*: Whole kidney lysates from three mice per group were subjected to immunoblot analysis with antibodies against Nrf2, NQO1, γ-GCS, and β-actin. The experiments were repeated three times, and one representative blot is shown (*left panel*). The intensity of bands from replicate immunoblots was quantified and plotted (*right panel*, *bar graphs*). *$P < 0.05$ compared with control. *B*: Fixed kidney tissues were stained with antibodies against Nrf2, NQO1, and γ-GCS. Representative images from each group showed a slight induction of Nrf2 and downstream targets upon STZ injection. Treatment with SF and CA further induced the Nrf2 pathway in $Nrf2^{+/+}$ only. *C*: 8-oxo-dG staining assessed oxidative damage in the kidney, and a representative image is provided. *D*: Urine collected at the last 24 h of the experiment was used for measurement of urinary 8-oxo-dG. STZ injection caused significant DNA damage that was attenuated by treatment with SF and CA in $Nrf2^{+/+}$ only. Data are expressed as mean ± SD ($n = 3$). *$P < 0.05$ compared with control. #$P < 0.05$ dietary treatment compared with STZ alone. (A high-quality color representation of this figure is available in the online issue.)

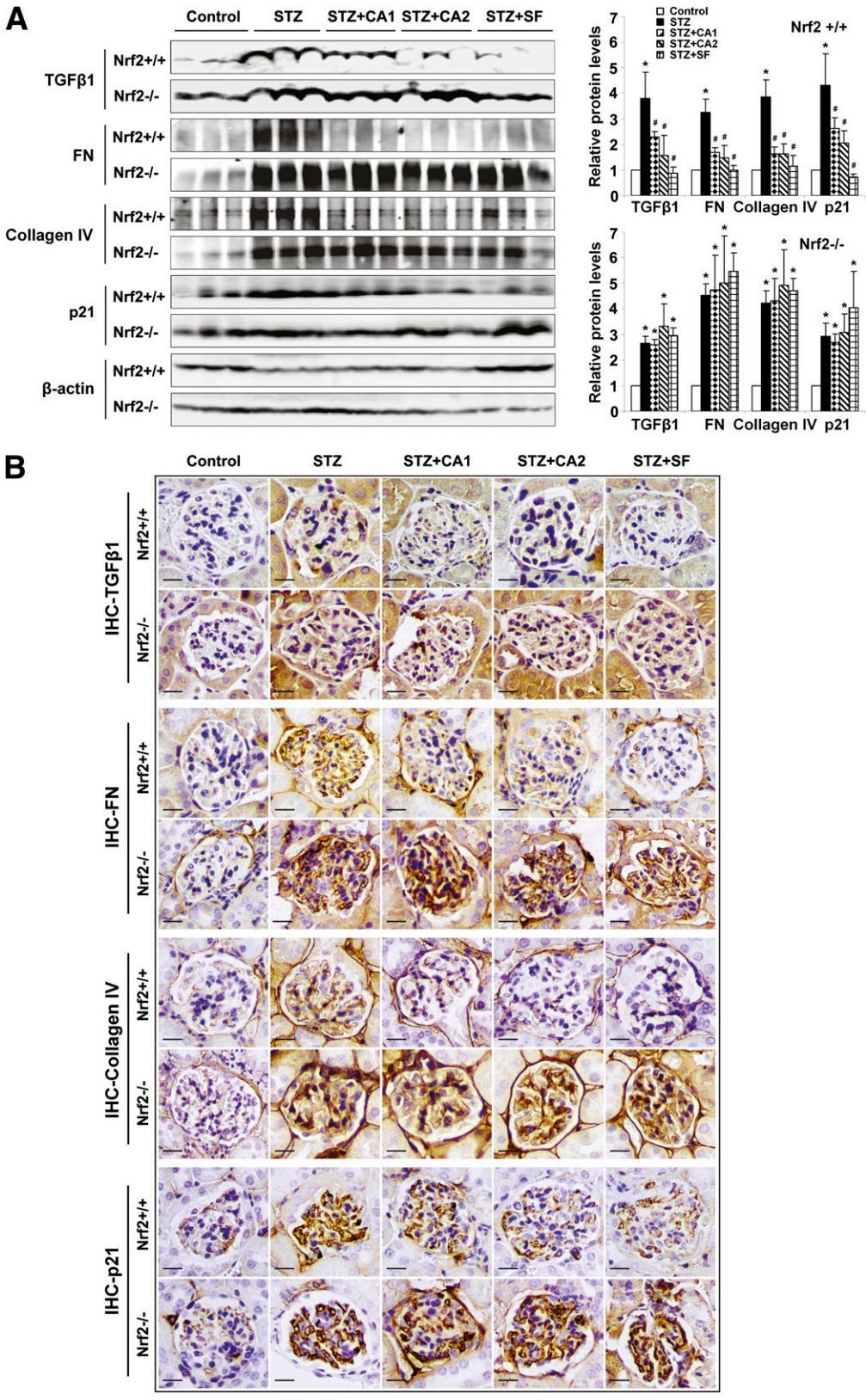

FIG. 4. Activation of Nrf2 reduces TGF-β1, ECM deposition, and p21 expression. *A*: Immunoblot analysis was performed on lysates from whole kidney (*left panel*), and band intensities were quantified (*right panel*, *bar graphs*) and reported as relative expression to control animals. STZ injection increased TGF-β1, FN, collagen IV, and p21 expression. Treatment with SF and CA reduced this expression in Nrf2$^{+/+}$ only. *B*: Fixed kidney tissue was analyzed by IHC. STZ injection increased staining of the glomeruli for TGF-β1, FN, collagen IV, and p21. Treatment with SF and CA reduced expression of TGF-β1, FN, collagen IV, and p21 in Nrf2$^{+/+}$ only. Data are expressed as mean ± SD (n = 3). *P < 0.05 compared with control. #P < 0.05 dietary treatment compared with STZ alone. (A high-quality color representation of this figure is available in the online issue.)

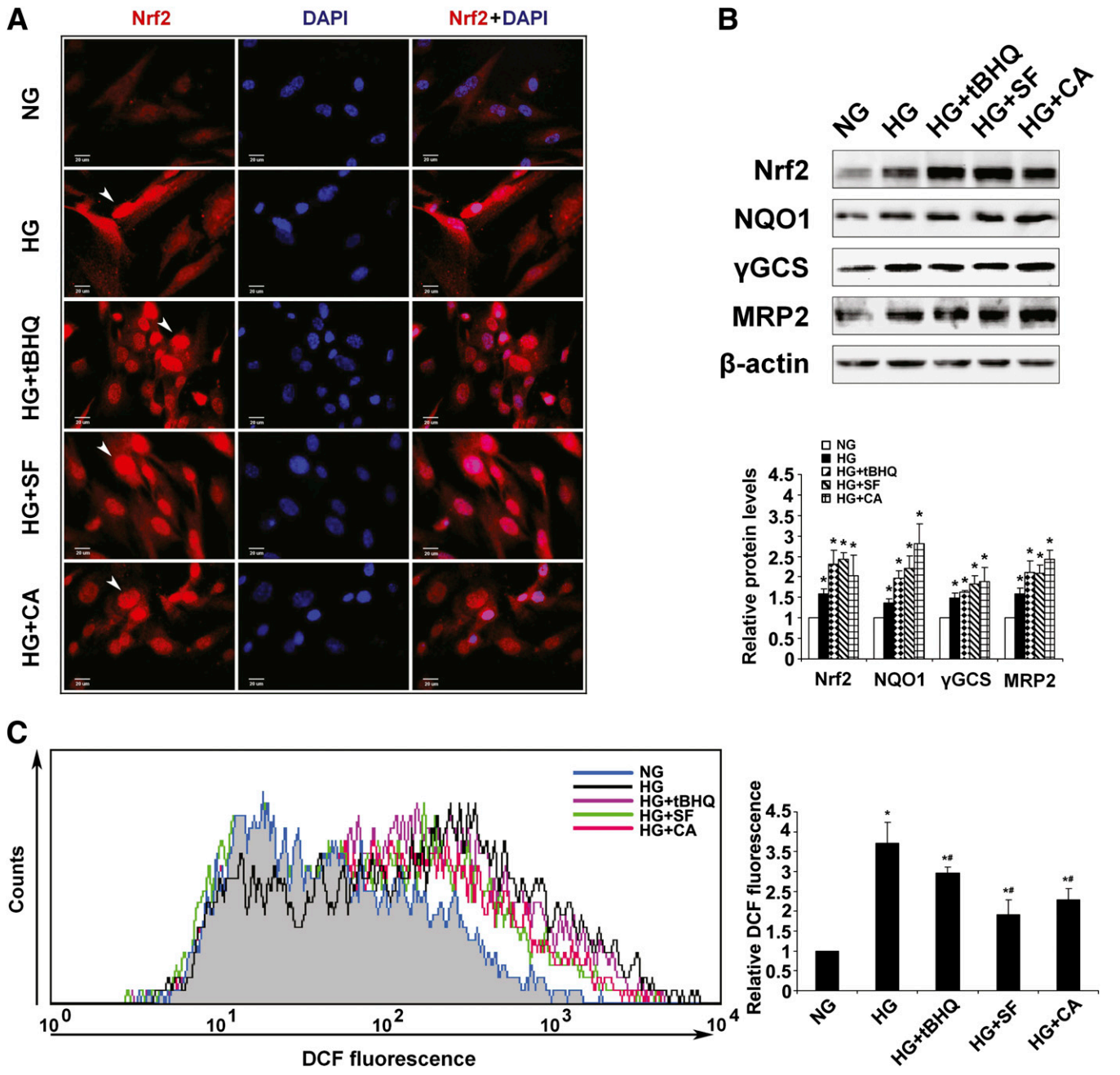

FIG. 5. Activation of Nrf2 diminishes mesangial ROS generation under hyperglycemic conditions. *A*: Nrf2 expression and localization were assessed in HRMCs incubated in NG, HG, HG+tBHQ, HG+SF, or HG+CA DMEM media for 48 h. Incubation in HG as well as treatment with an Nrf2 activator increased Nrf2 staining intensity and localization to the nucleus. *B*: Protein expression of Nrf2 and downstream targets was analyzed in HRMCs incubated in NG, HG, HG+tBHQ, HG+SF, or HG+CA DMEM media for 48 h. Representative Western blots and the relative quantification are provided. *C*: ROS levels in HRMCs incubated in NG, HG, HG+tBHQ, HG+SF, or HG+CA DMEM media are reported. HG stimulated ROS in HRMCs, whereas cotreatment with an Nrf2 activator for 48 h significantly reduced ROS. Data are expressed as mean ± SD ($n = 3$). *$P < 0.05$ compared with NG group. #$P < 0.05$ Nrf2 activators compared with HG alone. DCF, dichlorodihydrofluorescein diacetate. (A high-quality color representation of this figure is available in the online issue.)

were analyzed. Consistent with our in vivo data, hyperglycemia upregulated TGF-β1, FN, collagen IV, and p21 in HRMCs, which was suppressed by treatment with tBHQ, SF, or CA (Fig. 7*A*). Next, the functional contribution of the cell cycle regulator, p21, in mesangial cell growth inhibition and hypertrophy was investigated. Knockdown of p21 expression by transient transfection with p21-siRNA reduced the protein level of p21 and recovered the growth rate of HRMCs in HG media to that of NG conditions (Fig. 7*B*), while control siRNA had no effects on HRMC growth (Fig. 7*B*). Furthermore, hypertrophy of HRMCs growing in HG was no longer observed when expression of p21 was reduced by siRNA (Fig. 7*C*), indicating p21 controls mesangial growth inhibition and hypertrophy.

To further confirm the negative regulation of Nrf2 on TGF-β1 and its downstream response, endogenous Nrf2 levels were modulated either by Nrf2-siRNA or by siRNA to Keap1, a negative regulator of Nrf2. As expected, Nrf2 levels were reduced by Nrf2-siRNA and increased by Keap1-siRNA (Fig. 7*D*). The resulting effects of Nrf2 modulation display

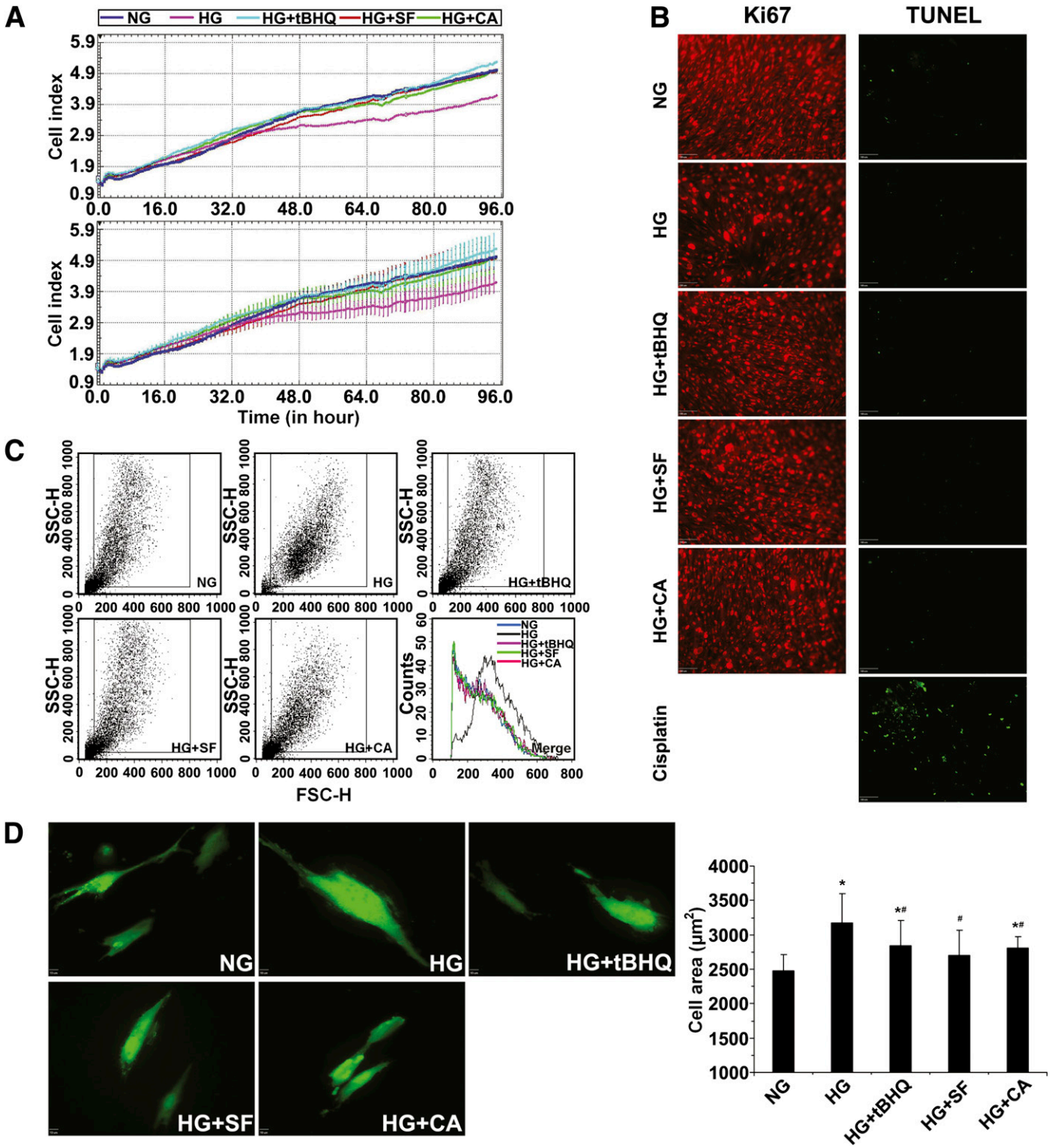

FIG. 6. High glucose–mediated mesangial cell growth inhibition and hypertrophy can be reversed by activation of Nrf2. *A*: Cell growth of HRMCs incubated in NG, HG, HG+tBHQ, HG+SF, or HG+CA DMEM media was monitored in real-time for 96 h (*upper panel* = average; *lower panel* = average with error). *B*: Cell death and proliferation were assessed by transferase-mediated dUTP nick-end labeling (TUNEL) assay (positive control is treated with cisplatin at 18 μmol/L for 24 h) or Ki67 immunolabeling. HG media induced cell growth inhibition, which was alleviated by coculture with an Nrf2 activator. *C*: Cell size of HRMCs incubated in NG, HG, HG+tBHQ, HG+SF, or HG+CA DMEM media for 96 h was measured by forward light scatter/flow cytometry. Incubation in HG media induced cellular hypertrophy that was reduced with an Nrf2 activator. *D*: Cell area is reported from GFP-transfected HRMCs incubated in NG, HG, HG+tBHQ, HG+SF, or HG+CA DMEM media for 48 h. Total cell area increased with HG conditions but was significantly reduced in the presence of an Nrf2 activator. Data in *D* are expressed as mean ± SD (n = 100). *P < 0.05 compared with NG group. #P < 0.05 Nrf2 activators compared with HG alone. FSC-H, forward scatter. SSC-H, side scatter. (A high-quality color representation of this figure is available in the online issue.)

a negative Nrf2 regulation of TGF-β1 and its downstream effectors including FN, collagen IV, and p21. Specifically, downregulation of Nrf2 resulted in enhanced expression of these proteins, whereas upregulation of Nrf2 reduced expression of the TGF-β1 pathway under both NG and HG media (Fig. 7*D*). Taken together, these results suggest that Nrf2 activation is able to confer renal protection in diabetic conditions through blockage of the TGF-β1 downstream

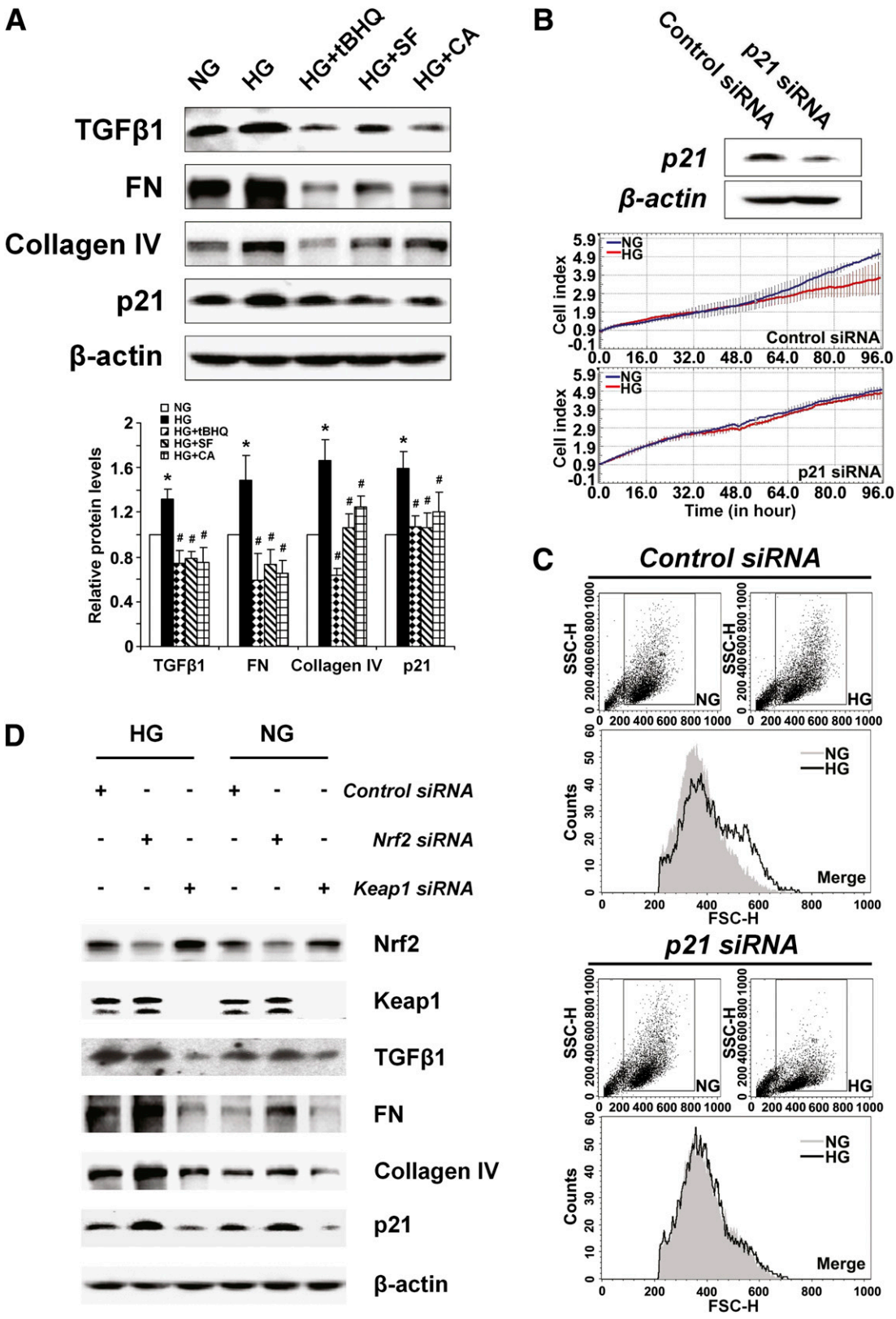

FIG. 7. Blockage of TGF-β1 by Nrf2 activation alleviates ECM production and p21-mediated mesangial cell growth inhibition and hypertrophy. *A*: Expression of TGF-β1 and downstream proteins was assessed by immunoblot analysis in HRMCs incubated in NG, HG, HG+tBHQ, HG+SF, or HG+CA DMEM media for 48 h (*upper panel*). Relative protein expression averaged over triplicate experiments are presented in bar graphs (*lower panel*). HG increased TGF-β1, FN, collagen IV, and p21. Coculture with an Nrf2 activator prevented increase of these proteins. *$P < 0.05$ compared to NG group. #$P < 0.05$ Nrf2 activators compared to HG alone (*bar graph*). *B*: Representative immunoblots and live cell growth curves from HRMCs transfected with p21-siRNA. Knockdown of p21 rescues growth inhibition induced by HG conditions. *C*: Representative images from flow cytometry analysis of forward light scatter analysis. Knockdown of p21 reduces HG-induced hypertrophy in HRMCs. *D*: Representative immunoblots from HRMCs transfected with control siRNA, Nrf2-siRNA, or Keap1-siRNA. Knockdown of Keap1 and Nrf2 illustrate the Nrf2-dependent repression of TGF-β1, ECM proteins, and p21 under both normal and hyperglycemic conditions. FSC-H, forward scatter. SSC-H, side scatter. (A high-quality color representation of this figure is available in the online issue.)

response, specifically by reducing ECM overproduction and p21-mediated growth inhibition and hypertrophy.

DISCUSSION

In the current study, the therapeutic potential of dietary Nrf2 activators in diabetic nephropathy is clearly demonstrated both in vivo and in vitro. Treatment with Nrf2 activators, SF, or CA, significantly reduced common metabolic disorder indices associated with diabetes, including hyperglycemia, polydipsia, polyuria, and weight loss. In the kidney, SF or CA treatment retarded pathological characteristics of diabetic nephropathy including oxidative damage, albuminuria, renal hypertrophy, ECM deposition, and thickening of basement membranes. All these effects were only observed in $Nrf2^{+/+}$ mice, indicating that the beneficial effects of SF or CA is derived from specific activation of the Nrf2 pathway. Furthermore, treatment with CA, SF, and tBHQ is able to protect mesangial cells from high glucose–induced alterations such as ROS and ECM production, cell growth inhibition, and hypertrophy in vitro, which is likely through Nrf2's negative regulation of TGF-β1 and p21.

In addition to demonstrating the therapeutic potential of SF or CA in suppressing diabetic nephropathy pathogenesis, we also sought the mechanism by which Nrf2 activation by these compounds is able to provide beneficial effects. One contributing factor is possibly the mild reduction of blood glucose in SF- or CA-treated $Nrf2^{+/+}$ mice. Importantly, Nrf2 activation had no effects on insulin levels, indicating that the observed reduction of blood glucose is insulin independent. Recently it was reported that gluconeogenesis and glycolysis are altered in $Nrf2^{-/-}$ mice (32) suggesting that the reduction of blood glucose in our SF- or CA-treated $Nrf2^{+/+}$ mice may be partially due to Nrf2-mediated glucose metabolism and glycogen formation in their livers. Alternatively, administration of SF or CA may affect insulin sensitivity in peripheral tissues, thereby altering systemic insulin resistance. Literature supports the notion of at least CA influencing glucose uptake in fibroblasts (33); and Nrf2 was shown to be central in the acquisition of insulin resistance induced by oxidative stress in cardiomyocytes (34). Future studies should include closer inspection of the effects of SF and CA on the major peripheral tissues contributing to insulin resistance in diabetes (i.e., skeletal muscle and adipocytes).

Another contributing factor to Nrf2 protection in diabetic nephropathy might be the Nrf2-dependent antioxidant response. The role of oxidative stress in the pathogenesis of diabetic nephropathy has gained increasing attention in the field (3,35). Previously, we detected oxidative damage in the glomeruli of both human diabetic nephropathy patients and STZ-injected mice (11). In the current study, SF or CA treatment significantly reduced oxidative damage in the glomerular tissues and urine of STZ-treated $Nrf2^{+/+}$ mice. Collectively, these results indicate the importance of the Nrf2-dependent antioxidant response in neutralizing ROS and alleviating oxidative damage in the kidney.

Nrf2-mediated protection in diabetic nephropathy may also rely on the negative regulation of Nrf2 on TGF-β1, a major profibrotic mediator of diabetic nephropathy. We have previously shown a negative association between Nrf2 and TGF-β1 promoter activity (11), however the precise mechanism remains unknown. Here, Nrf2 activation by SF or CA decreased protein levels of TGF-β1 in the kidney of diabetic $Nrf2^{+/+}$ mice and in HRMCs growing in HG media in vitro. Subsequently, we found that the beneficial effects of Nrf2 activation through TGF-β1 downregulation are due to suppression of both ECM production and p21 expression. ECM overproduction is a hallmark of diabetic nephropathy, and the function of TGF-β1 signaling ECM production is well established (rev. in (36,37). Alterations in the rate of proliferation and enlargement of renal mesangial cells are other typical features in early diabetic nephropathy, and upregulation of p21 by high glucose or other factors is associated with mesangial hypertrophy in vitro and in vivo (38–41). A critical role of p21 in mesangial hypertrophy was demonstrated by the fact that diabetic $p21^{-/-}$ mice do not develop glomerular hypertrophy (39,42). Interestingly, these $p21^{-/-}$ mice exhibited no alterations in their histology or function of the kidney, providing evidence that chronic decrease in p21 through Nrf2 activation may not be detrimental in long-term therapies.

Recently, several attempts have been made at using Nrf2 activators as treatment for diabetes. Specific to the kidney, treatment with bardoxolone of type 2 diabetes patients having chronic kidney disease elicited significant improvements in the estimated glomerular filtration rate with mild to moderate side effects (20,43). Additionally, activation of Nrf2 with SF in cultured microvascular endothelial cells protected them from the biochemical dysfunction induced by hyperglycemia (21). Alternate therapies that addressed triosephosphate accumulation resulting from hyperglycemia also showed that high doses of thiamine reduced albuminuria, ROS, and dyslipidemia without reducing circulating glucose levels after STZ-induced diabetes (44,45). Indeed, diabetic nephropathy is a multifaceted disease with several contributing factors that are both systemic and local to the kidney, making combination therapy or the discovery of an equally versatile treatment essential.

Collectively, our findings indicate that the therapeutic benefit of Nrf2 activation in diabetic nephropathy is multifactorial. In addition to its antioxidant function, Nrf2 also negatively regulates TGF-β1, ECM, and p21 expression. The reported results provide convincing experimental evidence that dietary compounds targeting Nrf2 activation can be used therapeutically to improve metabolic disorder and relieve kidney damage induced by diabetes. This study lays the foundation for clinical evaluation and ultimately the development of new Nrf2 activators in therapeutic use to prevent the onset and progression of diabetic nephropathy.

ACKNOWLEDGMENTS

This study was supported by grants ES015010 (National Institutes of Health) and RSG-07-154 (American Cancer Society) (to D.D.Z.) and National Natural Science Foundation of China (number 30700384) (to H.Z.).

No potential conflicts of interest relevant to this article were reported.

H.Z. and W.W. researched data. H.Z., S.A.W., and D.D.Z. wrote the manuscript. G.T.W., P.K.W., and D.F. contributed to discussion and provided critical reagents.

The authors would like to thank Tony Day for his contributions to electron microscopy services and Wade Chew and the Arizona Cancer Center Analytical Core Shared Service for assistance with urinary analysis.

REFERENCES

1. Dronavalli S, Duka I, Bakris GL. The pathogenesis of diabetic nephropathy. Nat Clin Pract Endocrinol Metab 2008;4:444–452
2. Kanwar YS, Sun L, Xie P, Liu FY, Chen S. A glimpse of various pathogenetic mechanisms of diabetic nephropathy. Annu Rev Pathol 2011;6:395–423

3. Kashihara N, Haruna Y, Kondeti VK, Kanwar YS. Oxidative stress in diabetic nephropathy. Curr Med Chem 2010;17:4256–4269
4. Shankland SJ, Scholey JW, Ly H, Thai K. Expression of transforming growth factor-beta 1 during diabetic renal hypertrophy. Kidney Int 1994;46:430–442
5. Yamamoto T, Nakamura T, Noble NA, Ruoslahti E, Border WA. Expression of transforming growth factor beta is elevated in human and experimental diabetic nephropathy. Proc Natl Acad Sci USA 1993;90:1814–1818
6. Sharma K, Jin Y, Guo J, Ziyadeh FN. Neutralization of TGF-beta by anti-TGF-beta antibody attenuates kidney hypertrophy and the enhanced extracellular matrix gene expression in STZ-induced diabetic mice. Diabetes 1996;45:522–530
7. Ziyadeh FN. Mediators of diabetic renal disease: the case for TGF-beta as the major mediator. J Am Soc Nephrol 2004;15(Suppl. 1):S55–S57
8. Lau A, Villeneuve NF, Sun Z, Wong PK, Zhang DD. Dual roles of Nrf2 in cancer. Pharmacol Res 2008;58:262–270
9. Johnson JA, Johnson DA, Kraft AD, et al. The Nrf2-ARE pathway: an indicator and modulator of oxidative stress in neurodegeneration. Ann N Y Acad Sci 2008;1147:61–69
10. Rangasamy T, Guo J, Mitzner WA, et al. Disruption of Nrf2 enhances susceptibility to severe airway inflammation and asthma in mice. J Exp Med 2005;202:47–59
11. Jiang T, Huang Z, Lin Y, Zhang Z, Fang D, Zhang DD. The protective role of Nrf2 in streptozotocin-induced diabetic nephropathy. Diabetes 2010;59:850–860
12. Kensler TW, Wakabayashi N, Biswal S. Cell survival responses to environmental stresses via the Keap1-Nrf2-ARE pathway. Annu Rev Pharmacol Toxicol 2007;47:89–116
13. Kensler TW, Curphey TJ, Maxiutenko Y, Roebuck BD. Chemoprotection by organosulfur inducers of phase 2 enzymes: dithiolethiones and dithiins. Drug Metabol Drug Interact 2000;17:3–22
14. Kanematsu S, Yoshizawa K, Uehara N, et al. Sulforaphane inhibits the growth of KPL-1 human breast cancer cells *in vitro* and suppresses the growth and metastasis of orthotopically transplanted KPL-1 cells in female athymic mice. Oncol Rep 2011;26:603–608
15. Moon EY, Lee MR, Wang AG, et al. Delayed occurrence of H-ras12V-induced hepatocellular carcinoma with long-term treatment with cinnamaldehydes. Eur J Pharmacol 2006;530:270–275
16. Ping Z, Liu W, Kang Z, et al. Sulforaphane protects brains against hypoxic-ischemic injury through induction of Nrf2-dependent phase 2 enzyme. Brain Res 2010;1343:178–185
17. Sussan TE, Rangasamy T, Blake DJ, et al. Targeting Nrf2 with the triterpenoid CDDO-imidazolide attenuates cigarette smoke-induced emphysema and cardiac dysfunction in mice. Proc Natl Acad Sci USA 2009;106:250–255
18. Wondrak GT, Villeneuve NF, Lamore SD, Bause AS, Jiang T, Zhang DD. The cinnamon-derived dietary factor cinnamic aldehyde activates the Nrf2-dependent antioxidant response in human epithelial colon cells. Molecules 2010;15:3338–3355
19. Yoh K, Hirayama A, Ishizaki K, et al. Hyperglycemia induces oxidative and nitrosative stress and increases renal functional impairment in Nrf2-deficient mice. Genes Cells 2008;13:1159–1170
20. Pergola PE, Raskin P, Toto RD, et al. Bardoxolone methyl and kidney function in CKD with type 2 diabetes. N Engl J Med 2011;365:327–336
21. Xue M, Qian Q, Adaikalakoteswari A, Rabbani N, Babaei-Jadidi R, Thornalley PJ. Activation of NF-E2-related factor-2 reverses biochemical dysfunction of endothelial cells induced by hyperglycemia linked to vascular disease. Diabetes 2008;57:2809–2817
22. Li H, Zhang L, Wang F, et al. Attenuation of glomerular injury in diabetic mice with tert-butylhydroquinone through nuclear factor erythroid 2-related factor 2-dependent antioxidant gene activation. Am J Nephrol 2011;33:289–297
23. Palsamy P, Subramanian S. Resveratrol protects diabetic kidney by attenuating hyperglycemia-mediated oxidative stress and renal inflammatory cytokines via Nrf2-Keap1 signaling. Biochim Biophys Acta 2011;1812:719–731
24. Song MY, Kim EK, Moon WS, et al. Sulforaphane protects against cytokine- and streptozotocin-induced beta-cell damage by suppressing the NF-kappaB pathway. Toxicol Appl Pharmacol 2009;235:57–67
25. Moi P, Chan K, Asunis I, Cao A, Kan YW. Isolation of NF-E2-related factor 2 (Nrf2), a NF-E2-like basic leucine zipper transcriptional activator that binds to the tandem NF-E2/AP1 repeat of the beta-globin locus control region. Proc Natl Acad Sci USA 1994;91:9926–9930
26. Jiang T, Huang Z, Chan JY, Zhang DD. Nrf2 protects against As(III)-induced damage in mouse liver and bladder. Toxicol Appl Pharmacol 2009;240:8–14
27. Renner T, Fechner T, Scherer G. Fast quantification of the urinary marker of oxidative stress 8-hydroxy-2′-deoxyguanosine using solid-phase extraction and high-performance liquid chromatography with triple-stage quadrupole mass detection. J Chromatogr B Biomed Sci Appl 2000;738:311–317
28. Weimann A, Belling D, Poulsen HE. Measurement of 8-oxo-2′-deoxyguanosine and 8-oxo-2′-deoxyadenosine in DNA and human urine by high performance liquid chromatography-electrospray tandem mass spectrometry. Free Radic Biol Med 2001;30:757–764
29. Wondrak GT, Cabello CM, Villeneuve NF, et al. Cinnamoyl-based Nrf2-activators targeting human skin cell photo-oxidative stress. Free Radic Biol Med 2008;45:385–395
30. Ren D, Villeneuve NF, Jiang T, et al. Brusatol enhances the efficacy of chemotherapy by inhibiting the Nrf2-mediated defense mechanism. Proc Natl Acad Sci U S A 2011;108:1433–1438
31. Lau A, Wang XJ, Zhao F, et al. A noncanonical mechanism of Nrf2 activation by autophagy deficiency: direct interaction between Keap1 and p62. Mol Cell Biol 2010;30:3275–3285
32. Aleksunes LM, Reisman SA, Yeager RL, Goedken MJ, Klaassen CD. Nuclear factor erythroid 2-related factor 2 deletion impairs glucose tolerance and exacerbates hyperglycemia in type 1 diabetic mice. J Pharmacol Exp Ther 2010;333:140–151
33. Plaisier C, Cok A, Scott J, et al. Effects of cinnamaldehyde on the glucose transport activity of GLUT1. Biochimie 2011;93:339–344
34. Tan Y, Ichikawa T, Li J, et al. Diabetic downregulation of Nrf2 activity via ERK contributes to oxidative stress-induced insulin resistance in cardiac cells in vitro and in vivo. Diabetes 2011;60:625–633
35. Singh DK, Winocour P, Farrington K. Oxidative stress in early diabetic nephropathy: fueling the fire. Nat Rev Endocrinol 2011;7:176–184
36. Ziyadeh FN. Different roles for TGF-beta and VEGF in the pathogenesis of the cardinal features of diabetic nephropathy. Diabetes Res Clin Pract 2008;82(Suppl. 1):S38–S41
37. Lee HS, Song CY. Differential role of mesangial cells and podocytes in TGF-beta-induced mesangial matrix synthesis in chronic glomerular disease. Histol Histopathol 2009;24:901–908
38. Abdel-Wahab N, Weston BS, Roberts T, Mason RM. Connective tissue growth factor and regulation of the mesangial cell cycle: role in cellular hypertrophy. J Am Soc Nephrol 2002;13:2437–2445
39. Fan YP, Weiss RH. Exogenous attenuation of p21(Waf1/Cip1) decreases mesangial cell hypertrophy as a result of hyperglycemia and IGF-1. J Am Soc Nephrol 2004;15:575–584
40. Kuan CJ, al-Douahji M, Shankland SJ. The cyclin kinase inhibitor p21WAF1, CIP1 is increased in experimental diabetic nephropathy: potential role in glomerular hypertrophy. J Am Soc Nephrol 1998;9:986–993
41. Monkawa T, Hiromura K, Wolf G, Shankland SJ. The hypertrophic effect of transforming growth factor-beta is reduced in the absence of cyclin-dependent kinase-inhibitors p21 and p27. J Am Soc Nephrol 2002;13:1172–1178
42. Al-Douahji M, Brugarolas J, Brown PA, Stehman-Breen CO, Alpers CE, Shankland SJ. The cyclin kinase inhibitor p21WAF1/CIP1 is required for glomerular hypertrophy in experimental diabetic nephropathy. Kidney Int 1999;56:1691–1699
43. Pergola PE, Krauth M, Huff JW, et al. Effect of bardoxolone methyl on kidney function in patients with T2D and Stage 3b-4 CKD. Am J Nephrol 2011;33:469–476
44. Babaei-Jadidi R, Karachalias N, Ahmed N, Battah S, Thornalley PJ. Prevention of incipient diabetic nephropathy by high-dose thiamine and benfotiamine. Diabetes 2003;52:2110–2120
45. Babaei-Jadidi R, Karachalias N, Kupich C, Ahmed N, Thornalley PJ. High-dose thiamine therapy counters dyslipidaemia in streptozotocin-induced diabetic rats. Diabetologia 2004;47:2235–2246